Supplementary Information (SI)

Dual-Axis Interfacial Engineering of Carbon Paper Hosts for Stable Anode-Less Lithium Metal Batteries

Authors

Sangjin Bae,[1,2,†] Gaeun Park,[1,†] Jihwan Byun,[1] Jisub Kim,[1] Jongmin Won,[1,2] Sujin Kim,[2] Minjun Je,[1] Heemin Kim,[2] Juhun Shin,[2] Jongseok Moon,[2] Jihoon Oh,[3,*] and Jang Wook Choi[1,3,4,*]

Affiliation

[1]School of Chemical and Biological Engineering and Institute of Chemical Process, Seoul National University, Seoul 08826, Republic of Korea

[2]R&D Center, Samsung SDI, Suwon-si 16678, Republic of Korea

[3]Institute for Battery Research Innovation (IBRI), Seoul National University, Seoul 08826, Republic of Korea

[4]Seoul National University Energy Initiative (SNUEI), Seoul National University, Seoul 08826, Republic of Korea

[†]These authors contributed equally

[*]Correspondence: jm9731@snu.ac.kr (J. O.), jangwookchoi@snu.ac.kr (J. W. C.)

Experimental

Preparation of Electrode

MgO-preSEI-CP was synthesized as follows. First, a homogeneous precursor solution was prepared by dissolving lithium acetate (LiOAc, Sigma-Aldrich, 5 g) and magnesium nitrate hexahydrate ($Mg(NO_3)_2 \cdot 6H_2O$, Sigma-Aldrich, 1 g) in 20 mL of dimethyl sulfoxide (DMSO, Sigma-Aldrich) under vigorous stirring. A piece of carbon paper (Toray, TGP-H-030), pre-cut to the desired dimensions, was then immersed in this solution for 1 h to ensure complete infiltration of its porous network.

Subsequently, the infiltrated carbon paper was dried at 80 °C for 6 h in an oven. The dried sample was subjected to a stepwise annealing process in a box furnace under an ambient atmosphere. The thermal protocol consisted of heating to 250 °C (1 h), 350 °C (1 h), and finally 450 °C (1 h), with controlled heating rates of 5 °C min^{-1} up to 350 °C and 3.33 °C min^{-1} thereafter. The resulting annealed product was used directly as the anode host without any further washing or treatment to preserve the surface structure and the composition/distribution of in-situ formed inorganic species on the CPs. For comparison, a control sample (preSEI-CP) was prepared using an identical procedure but omitting $Mg(NO_3)_2$ from the precursor solution.

Cathode electrodes were fabricated from a slurry containing $LiNi_{0.8}Co_{0.1}Mn_{0.1}O_2$ (NCM811, Posco Future M), Super P carbon black (Timcal), and polyvinylidene fluoride (PVdF, Kynar) binder in a weight ratio of 95:2.5:2.5. The PVdF binder was first dissolved in *N*-methyl-2-pyrrolidone (NMP) to form an 8 wt% solution. The active material, conductive carbon, and binder solution were then homogenized using a Thinky planetary mixer (AR-100). The resultant slurry was uniformly cast onto an aluminum current collector using a doctor blade, targeting an areal capacity of 3.5 mAh cm^{-2}. The coated electrodes were dried at 80 °C for 12 h and subsequently roll-pressed to a final thickness of approximately 85 μm (including the Al foil).

Cell Fabrication

Coin-type (CR2032) cells were assembled in an argon-filled glovebox (O_2 and H_2O < 0.1 ppm). A polypropylene (PP) separator (Celgard 2400) was employed, and 60 μL of electrolyte consisting of 3 M LiFSI in FSA was added to each cell. The working electrode was a 10 mm

diameter circular as-prepared CP host without additional compression. A 300 μm-thick lithium metal foil (12 mm diameter) served as the counter electrode in half-cell configurations, while the NCM811 cathodes described above were used as the counter electrodes in full-cell assemblies.

Characterizations

The surface and cross-sectional morphologies of the samples were examined using field-emission scanning electron microscopy (FE-SEM, JSM-7800F Prime, JEOL) equipped with an energy-dispersive X-ray spectroscopy (EDS) detector for elemental mapping. The chemical compositions of the anode hosts were analyzed by X-ray photoelectron spectroscopy (XPS, AXIS SUPRA, Shimadzu), while their crystal structures were characterized by X-ray diffraction (XRD, SmartLab, Korea I.T.S.). The Raman spectra of the host materials were recorded using a Raman spectrometer (DXR2xi, Thermo Fisher, USA). All characterization experiments were performed at the National Center for Inter-University Research Facilities (NCIRF).

All electrochemical measurements were carried out using a battery cycler (WBCS 3000, WonATech) at a constant temperature of 25 °C. For half-cell evaluation, the formation cycle was carried out by plating lithium in constant-current (CC) mode at 0.1C until the potential reached 0.1 V (vs. Li/Li^+), followed by a constant-voltage (CV) step maintained at 0.1 V until the current declined to 0.01C (1C = 3.5 mA cm^{-2}). Lithium stripping was subsequently performed under CC mode at the same rate up to 1.0 V (vs. Li/Li^+). After formation, the cells were cycled by depositing lithium at 0.33C for 3 h (equivalent to 3.5 mAh cm^{-2}) and stripping at the same current rate up to 1.0 V (vs. Li/Li^+). For full-cell configurations, galvanostatic cycling was performed within a voltage window of 3.7–4.3 V. Charging was conducted in constant-current–constant-voltage (CC–CV) mode at 0.33C, and discharging in CC mode at the same rate. The CV cutoff current was set to 0.033C. Before the main cycling test, a single formation cycle was applied to stabilize the electrode interfaces, consisting of CC charging at 0.1C followed by CV charging with a cutoff current of 0.01C, and subsequent CC discharging at 0.1C within the same voltage window.

Computational Details

The density functional theory (DFT) calculation of adsorption energies was performed with Quantum Espresso v.7.2. The exchange-correlation (XC) interactions of electrons were described by the generalized gradient approximation (GGA) with Perdew-Burke-Ernzerhof functional, and the projector-augmented wave (PAW) was used as the pseudopotentials. Additionally, Grimme's DFT-D3 correction was used to account for the long-range van der Waals forces. A graphene substrate was modeled as a 6 × 6 supercell monolayer, and graphene oxides as graphene monolayers with corresponding functional groups relaxed prior to the relaxation of Li-ion. MgO substrate was modeled using a rock-salt unit cell with 2.10 Å Mg-O bond length, truncated along (100), (110), or (111) plane to a 6 × 6 slab with 3 layers. PTFE (100) surface was modeled as planar zigzag chains packed in hcp structure with unit cell length of 5.664 Å. In all cases, 25 Å thick vacuum region in the direction perpendicular to the slab surface was kept to avoid interaction among periodic images. The energy cutoff threshold was set to 1.0×10^{-5} Ry and the force cutoff threshold for all atoms were set to 1.0×10^{-3} Ry/Bohr. The Brillouin zone was sampled with the 4×4×1 Monkhorst-Pack k-points grid. The adsorption energy (E_{ads}) of Li-ion onto a substrate was calculated by following formula:

$$E_{ads} = E(Li^+ + substrate) - E(Li^+) - E(substrate)$$

where $E(Li^+)$ is the energy of Li-ion, $E(substrate)$ is the energy of substrate after relaxation according to aforementioned criteria, and $E(Li^+ + substrate)$ is the combined energy of Li-ion relaxed on the substrate. Multiple initial positions of Li-ion was set to avoid convergence to local minima. The most negative value of E_{ads} was selected as the most stable adsorption geometry.

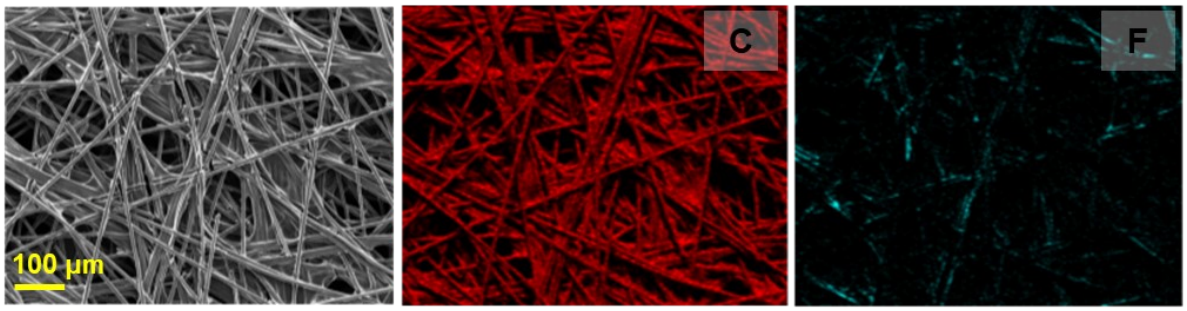

Fig. S1. SEM-EDS images of bare CP.

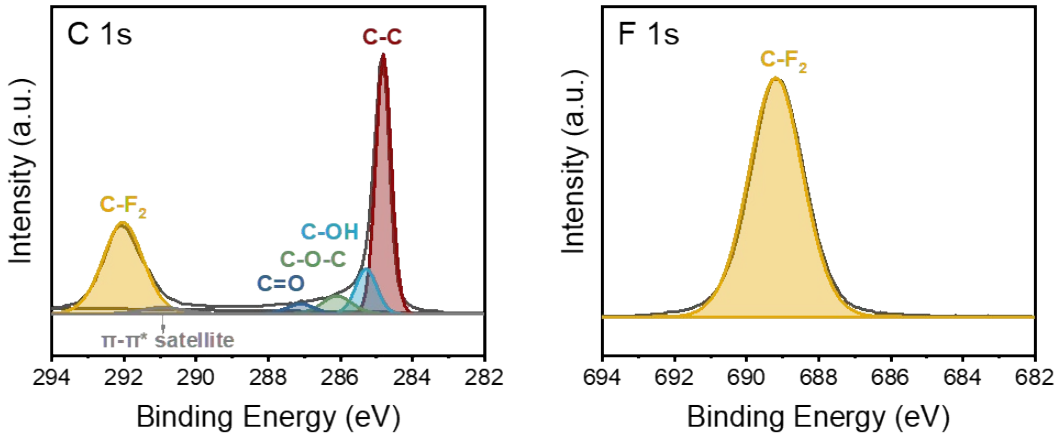

Fig. S2. XPS spectra of bare CP.

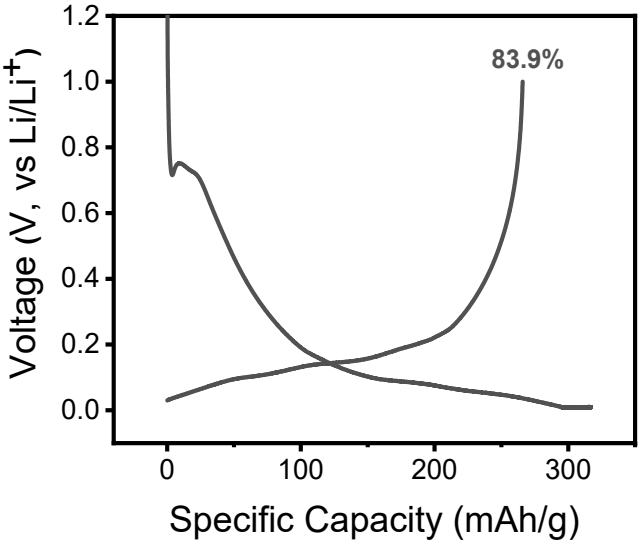

Fig. S3. 1st cycle half-cell voltage profile and corresponding Coulombic efficiency of CP.

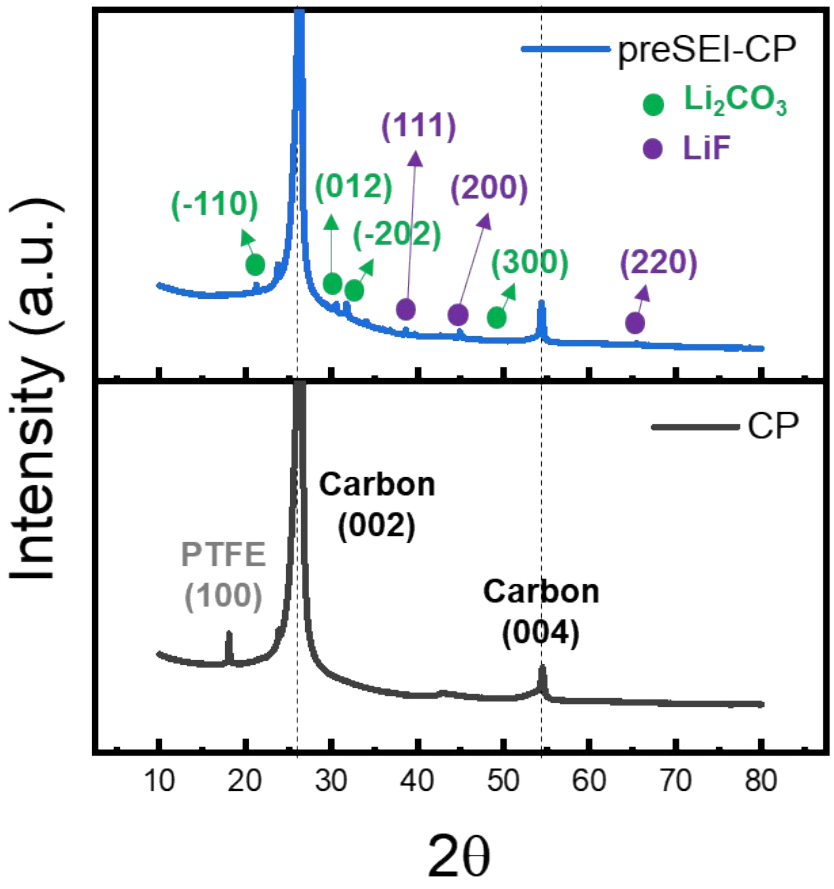

Fig. S4. XRD patterns of CP and preSEI-CP.

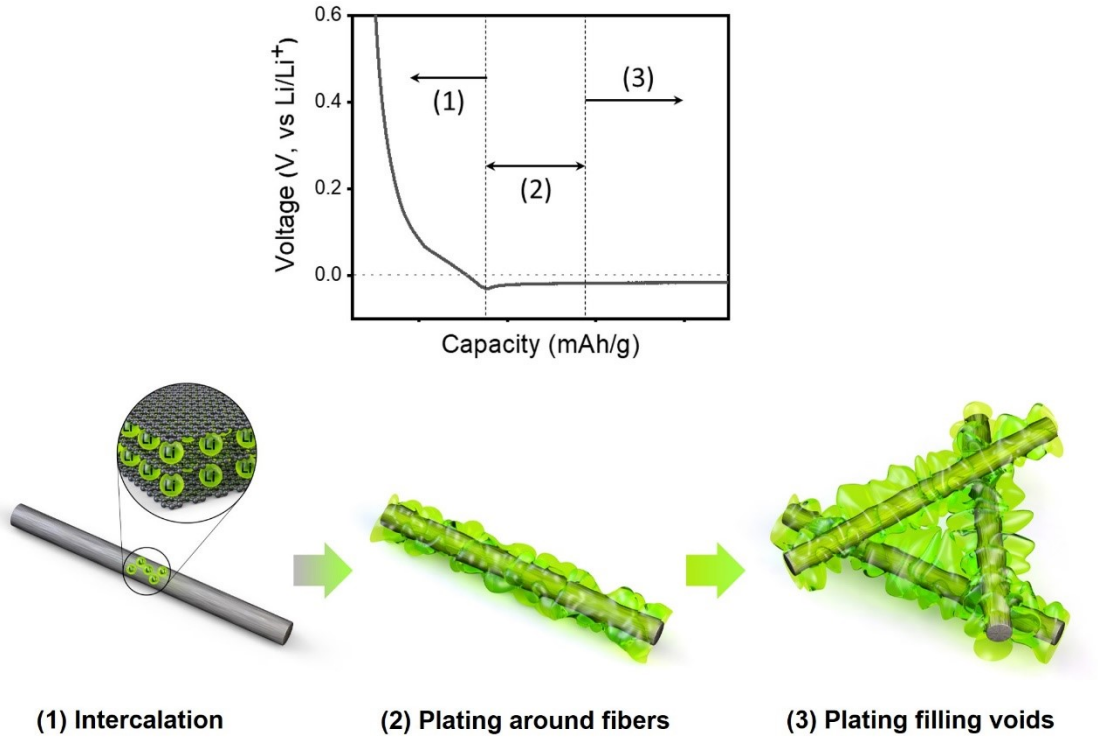

Fig. S5. Schematic illustration of lithiation steps of carbon fibers.

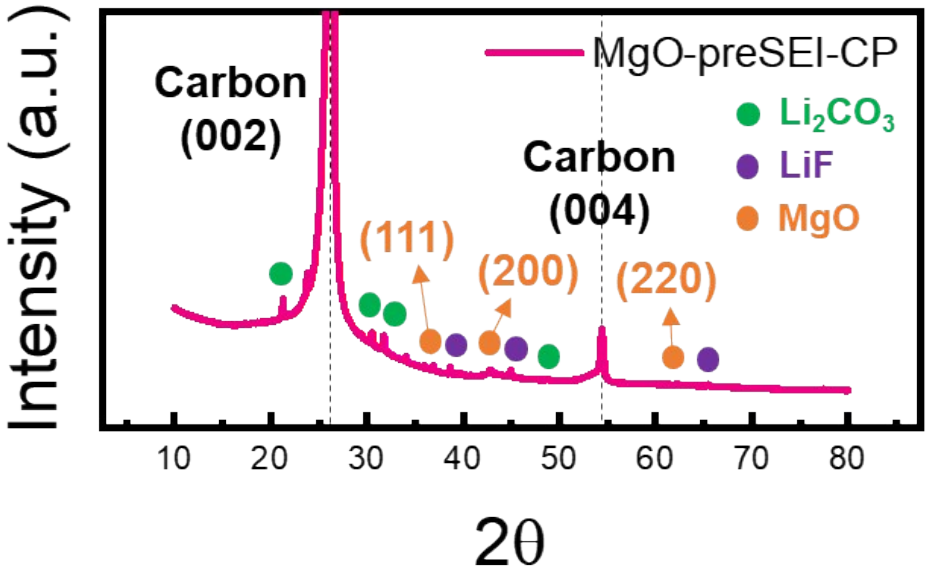

Fig. S6. XRD pattern of MgO-preSEI-CP.

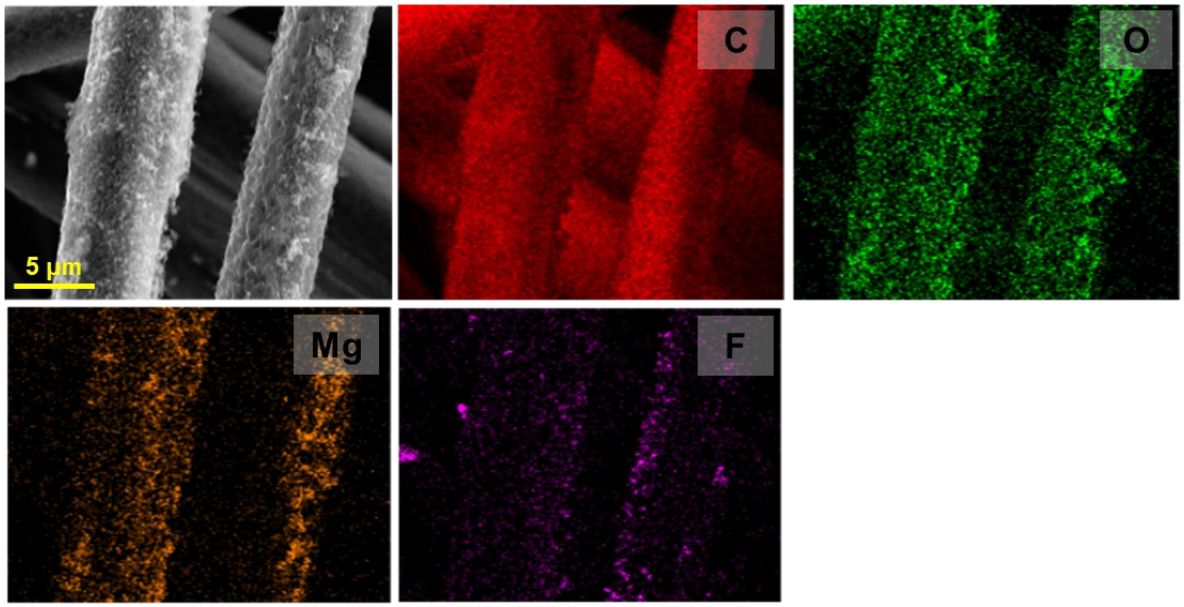

Fig. S7. High-magnification SEM image and corresponding EDS elemental maps of MgO-preSEI-CP, showing the spatial distributions of C, O, Mg, and F on individual carbon fibers.

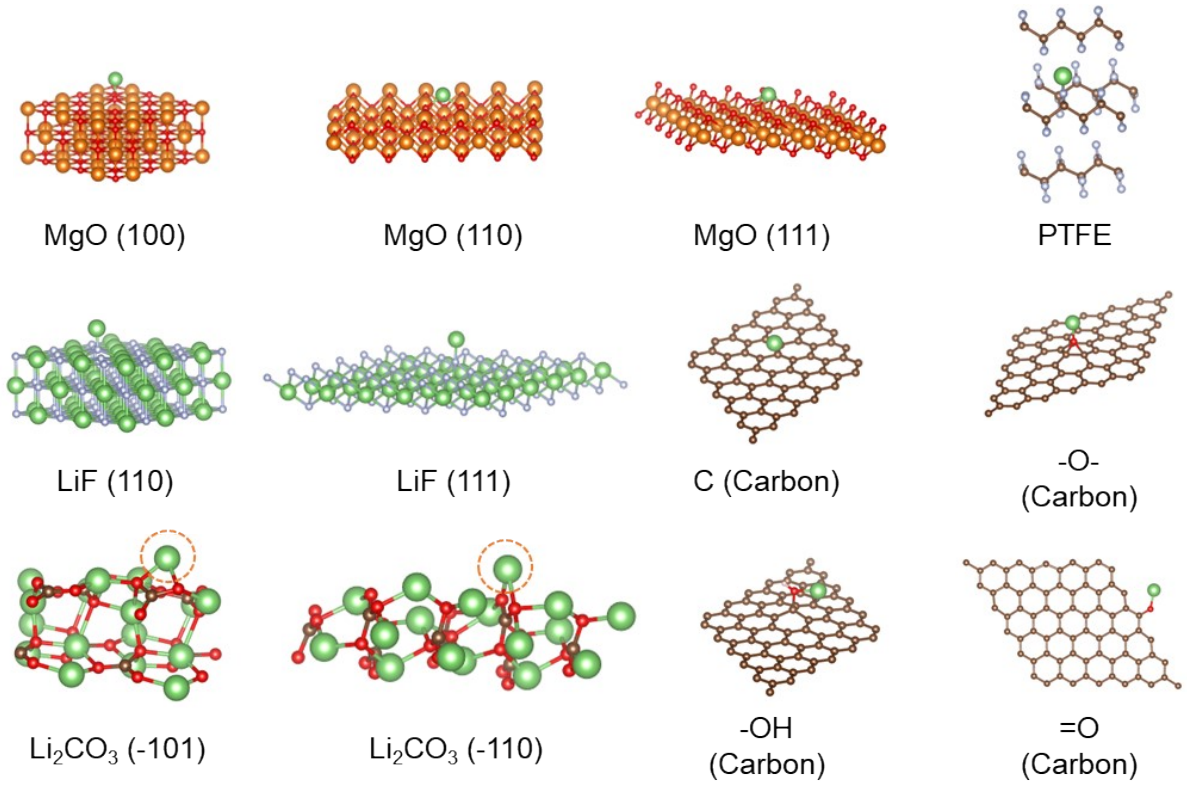

Fig. S8. Lowest-energy configurations of Li^+ adsorption on each substrate in DFT calculations.

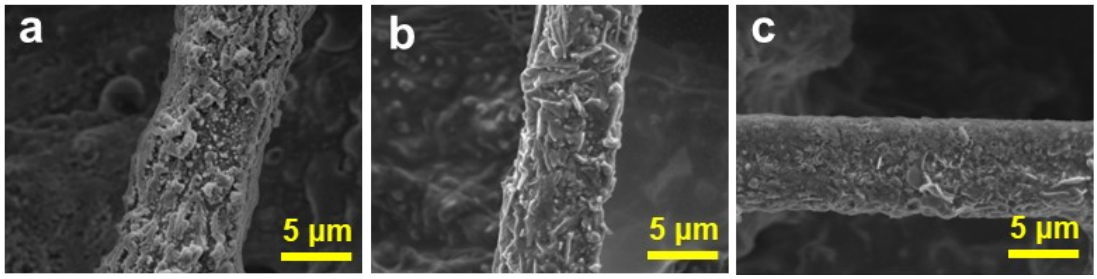

Fig. S9. High-magnification SEM images showing the initial lithium deposition morphology on individual carbon fibers of (a) CP, (b) preSEI-CP, and (c) MgO-preSEI-CP at a deposition capacity of 1.0 mAh cm^{-2}.

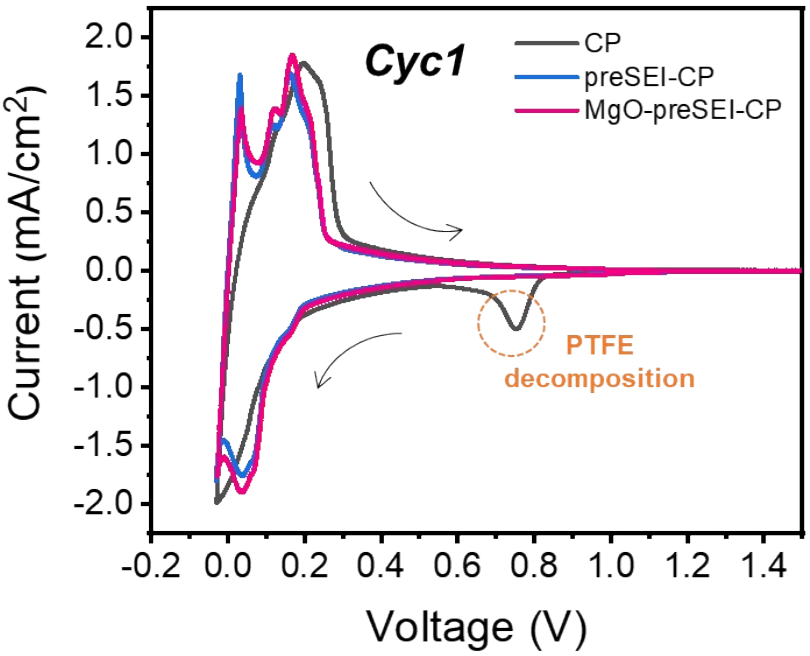

Fig. S10. Cyclic voltammetry curves of CP, preSEI-CP, and MgO-preSEI-CP in half-cells.

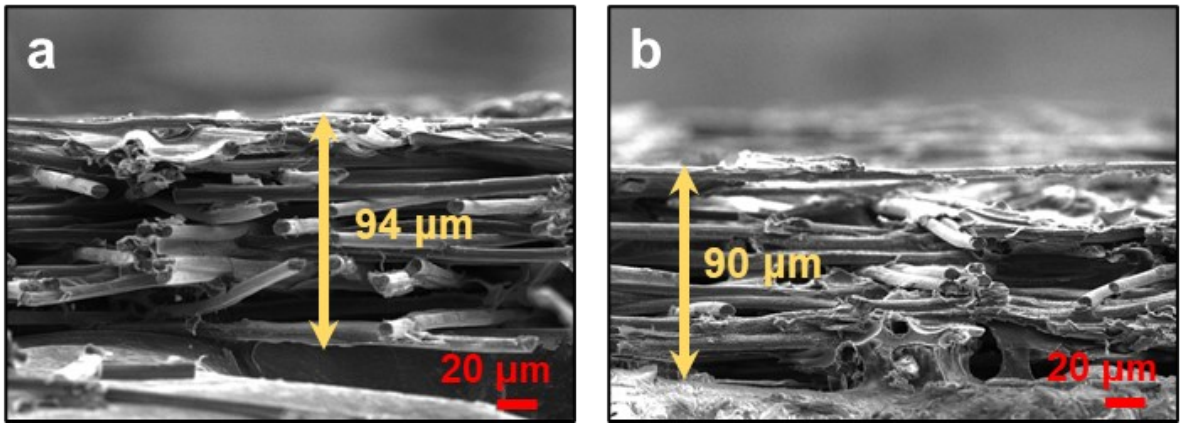

Fig. S11. Cross-sectional SEM images of (a) CP and (b) MgO-preSEI-CP in the pristine state.

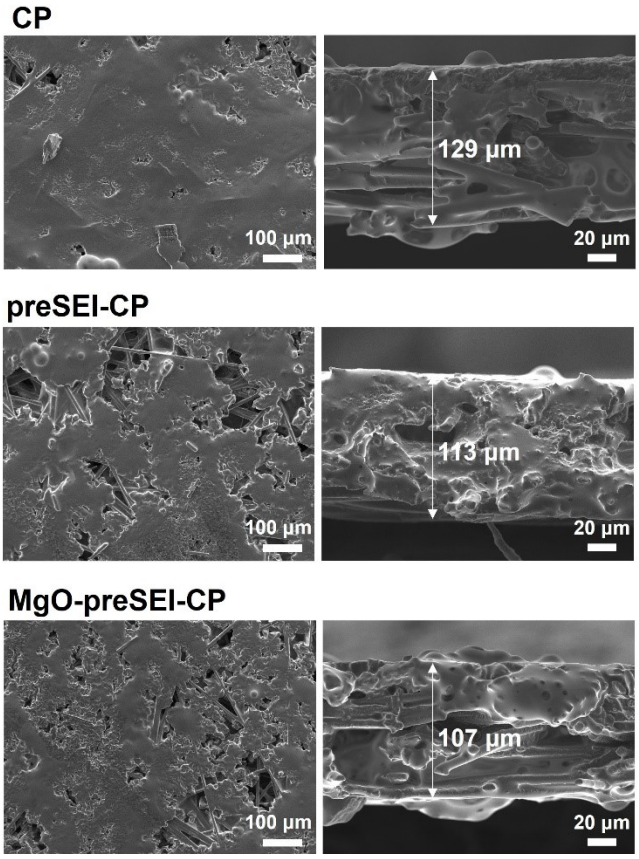

Fig. S12. Top surface and cross-sectional SEM images of the three CP hosts after the first Li plating at a current density of 2 mA cm^{-2}.

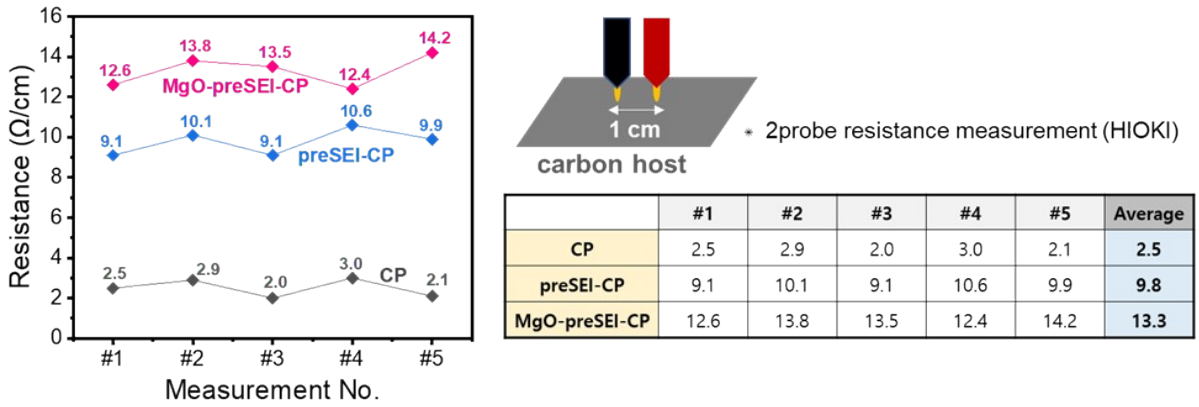

	#1	#2	#3	#4	#5	Average
CP	2.5	2.9	2.0	3.0	2.1	**2.5**
preSEI-CP	9.1	10.1	9.1	10.6	9.9	**9.8**
MgO-preSEI-CP	12.6	13.8	13.5	12.4	14.2	**13.3**

Fig. S13. Two-probe resistance measurements of CP, preSEI-CP, and MgO-preSEI-CP with a probe spacing of 1 cm. Five repeated measurements were performed for each sample, and the averaged resistance values are summarized.

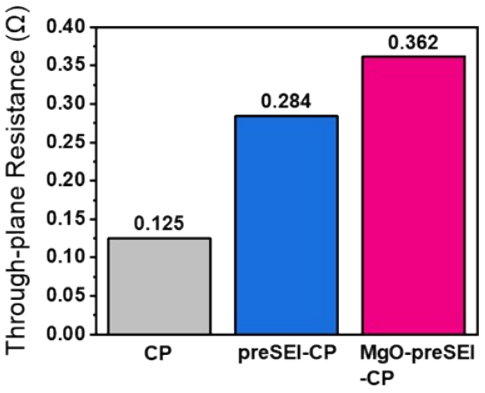

	#1	#2	#3	Average
CP	0.123	0.122	0.129	**0.125**
preSEI-CP	0.245	0.309	0.299	**0.284**
MgO-preSEI-CP	0.454	0.309	0.324	**0.362**

$$\sigma = \frac{1}{R} \cdot \frac{L}{A}$$

Conductivity (S/m)	
CP	2.39
preSEI-CP	0.90
MgO-preSEI-CP	0.79

Fig. S14. Two-probe through-plane resistance of three carbon host materials.

Note: Resistance values were measured using an Agilent 4284A LCR meter under a uniaxial pressure of 0.06 MPa with an AC perturbation of 10 mV at 1 kHz, with three repeated measurements and averaged. The corresponding through-plane electrical conductivity was calculated based on equation of $\sigma = L/(RA)$, where σ is the electrical conductivity (S m^{-1}), R is the measured through-plane resistance (Ω), L is the sample thickness (m), and A is the area of the sample (m^2).

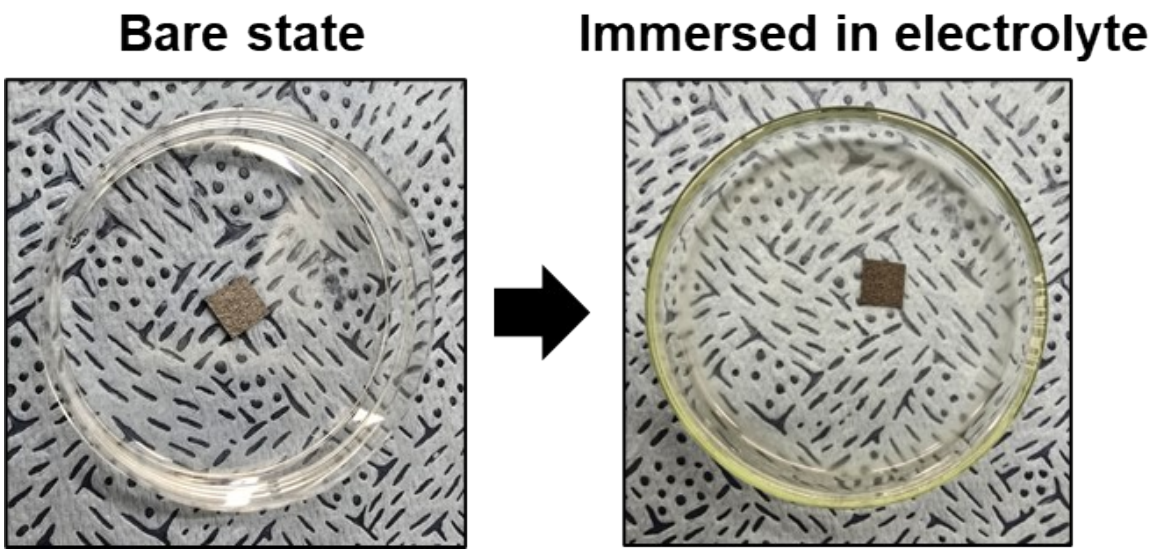

	Before (μg)	After (μg)	Increase (μg)	Increase (%)
CP	2170	11791	9621	443%
preSEI-CP	2161	24292	22131	1024%
MgO-preSEI-CP	2323	26858	24535	1056%

Fig. S15. Electrolyte wettability test of three host materials. Optical images show the samples before and after immersion in electrolyte. The mass of each sample before and after immersion, along with the corresponding electrolyte uptake and relative increase, are summarized in the table.

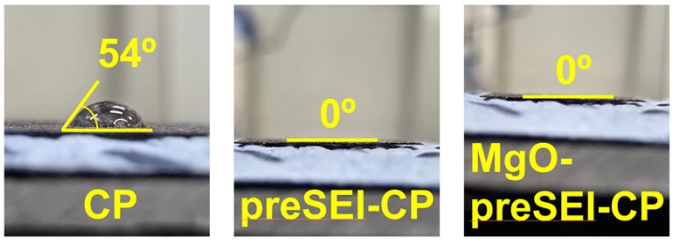

Fig. S16. Contact angle measurements of the three CP hosts, captured immediately after dispensing a 20 μL droplet of 3 M LiFSI in FSA electrolyte.

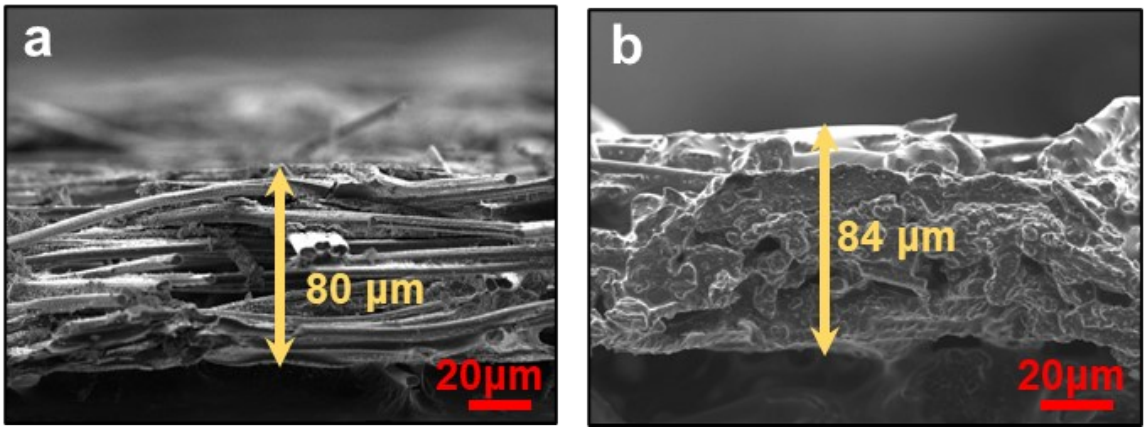

Fig. S17. The cross-sectional SEM images of preSEI-CP (a) at the pristine state and (b) after 3.5 mAh cm^{-2} Li electrodeposition.

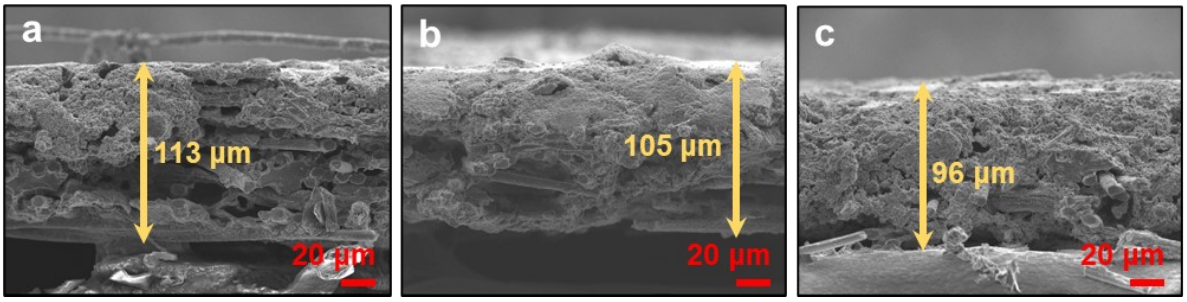

Fig. S18. Cross-sectional SEM images of (a) CP, (b) preSEI-CP, and (c) MgO-preSEI-CP after the 81th deposition cycle in half-cells.

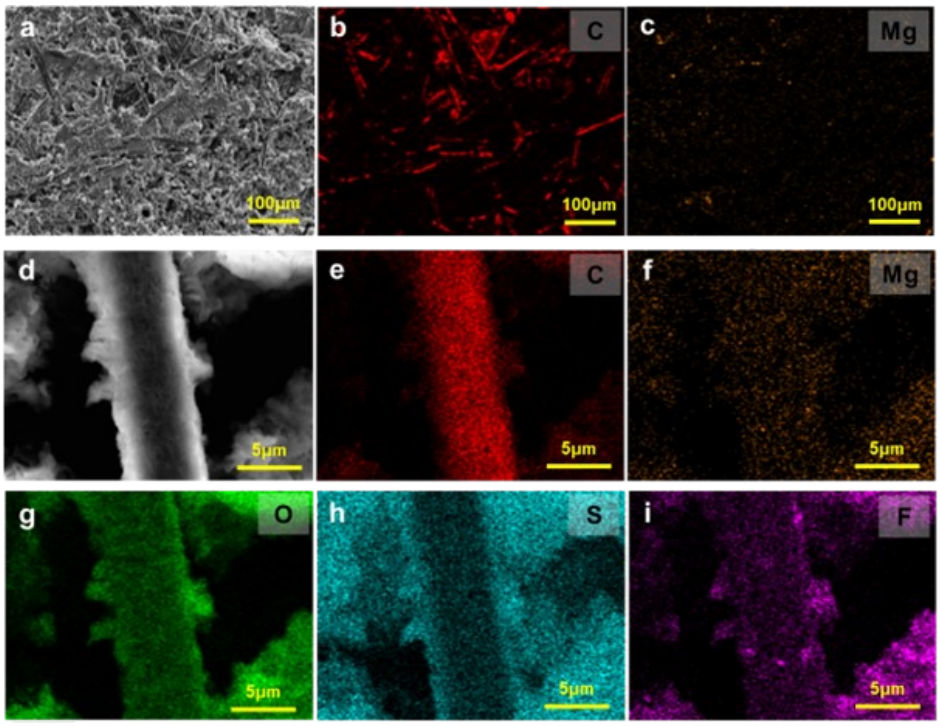

Fig. S19. Post-mortem SEM image and corresponding EDS elemental mappings of MgO-preSEI-CP after the 80th stripping cycle in half-cells, with (a-c) low and (d-i) high magnification.

a

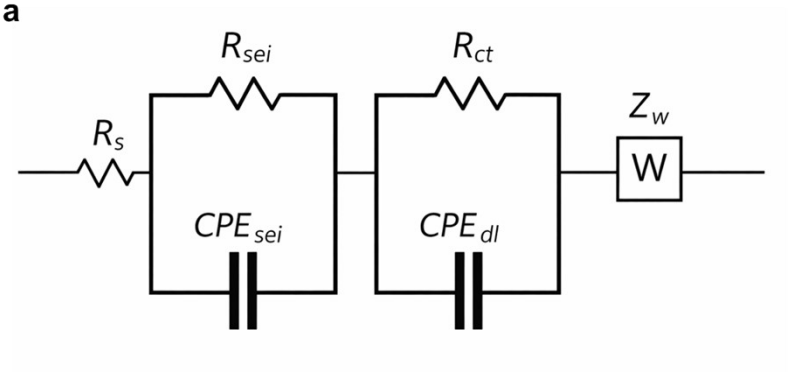

b

@cyc1	R_{sei}	R_{ct}	R_{sei} + R_{ct}
CP	22.4	215.3	237.7
preSEI-CP	4.6	14.0	18.6
MgO-preSEI-CP	10.2	12.6	22.8

c

@cyc80	R_{sei}	R_{ct}	R_{sei} + R_{ct}
CP	57.9	276.5	334.4
preSEI-CP	22.7	31.9	54.6
MgO-preSEI-CP	2.0	16.9	18.9

Fig. S20. (a) Equivalent circuit for EIS fitting and corresponding fitted resistance values (R_{sei} and R_{ct}) for CP, preSEI-CP, and MgO-preSEI-CP after (b) the 1st cycle and (b) the 80th cycle.

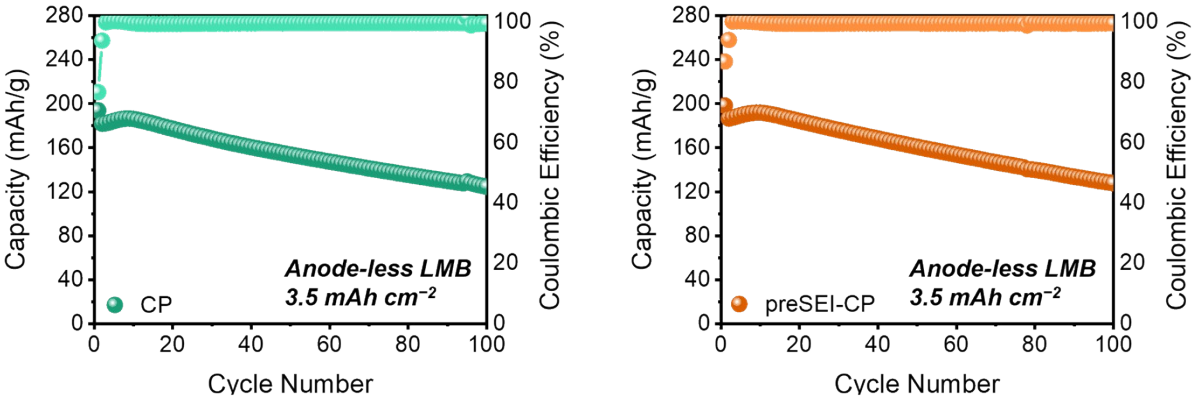

Fig. S21. Full-cell cycling performance of CP and preSEI-CP.

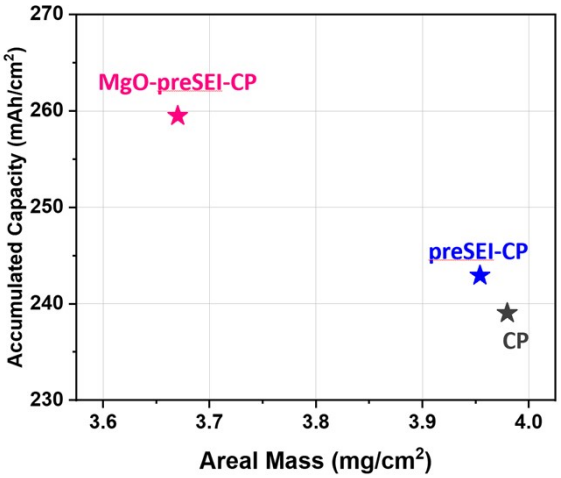

Fig. S22. Anode-less full-cell performance: accumulated capacities over 85 cycles plotted as a function of the areal mass of the host materials.

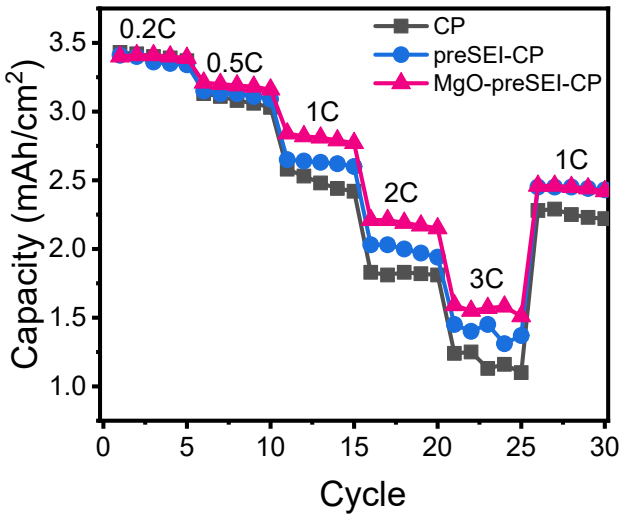

Fig. S23. Full-cell rate performances of CP, preSEI-CP and MgO-preSEI-CP (1C = 3.5 mA cm^{-2}).

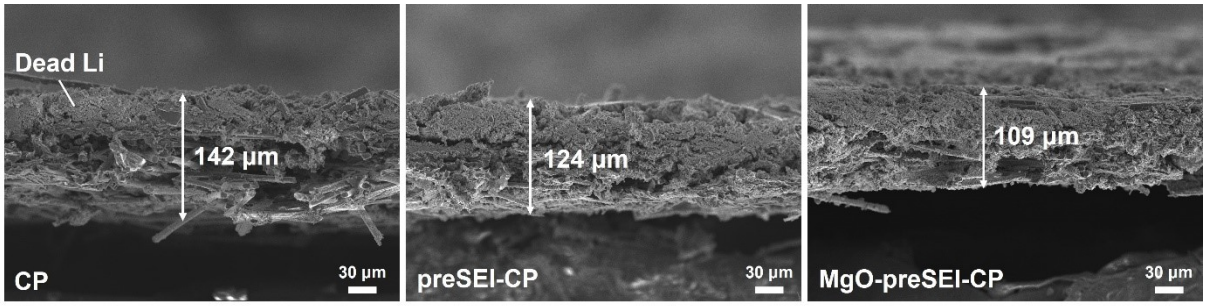

Fig. S24. Cross-sectional SEM images of the three CP hosts after 80 full-cell cycles.